The ER protein translocation channel subunit Sbh1 controls virulence of *Cryptococcus neoformans*

Felipe H. Santiago-Tirado[1,5], Thomas Hurtaux[1], Jennifer Geddes-McAlister[2], Duy Nguyen[3,6], Volkhard Helms[3], Tamara L. Doering[1]*, Karin Römisch[4] *

1 Department of Molecular Microbiology, Washington University Medical School, St. Louis, Missouri, USA; fsantiago@nd.edu; thomas.hurtaux@wustl.edu; doering@wustl.edu

2 Department of Molecular and Cellular Biology, University of Guelph, Ontario, Canada; jgeddesm@uoguelph.ca

3 Center for Bioinformatics, Faculty of Natural Sciences and Technology, Saarland University, Saarbruecken, Germany; volkhard.helms@ bioinformatik.uni-saarland.de

4 Department of Biology, Faculty of Natural Sciences and Technology, Saarland University, Saarbruecken, Germany; k.roemisch@mx.uni-saarland.de

5 Current address: Department of Biological Sciences, University of Notre Dame, Notre Dame, IN46556, USA

6 Current address: DKFZ Heidelberg, Germany; duy.nguyen@dkfz-heidelberg.de

* corresponding authors: k.roemisch@mx.uni-saarland.de
phone: +49-681-302 2704; ORCID ID 0000-0003-0415-6558

doering@wustl.edu
phone +1-314-747-5597; ORCID ID 0000-0002-5179-7393

Running title: Sbh1-dependence of *Cryptococcus neoformans* virulence (48 characters)

- KR was funded by core funding of the Saarland University. Work in the Doering lab was supported by NIH grants AI140979 and AI135012 to TLD. FHS also received support from NIH T32 grant AI007172 and a Postdoctoral Enrichment Program Award from the Burroughs Wellcome Fund. JGM is supported by the Canadian Foundation for Innovation (JELF #38798) and the Canadian Institutes for Health Research (Project Grant).VH was supported by Deutsche Forschungsgemeinschaft grant He3875/15-1.

- Data available on request from the authors. Proteomics data are deposited in PRIDE.
- The authors declare no conflict of interest.
- All animal studies were reviewed and approved by the Animal Studies Committee of Washington University School of Medicine and conducted according to the National Institutes of Health guidelines for housing and care of laboratory animals.

Abstract

The fungal pathogen *Cryptococcus neoformans* is distinguished by a cell wall-anchored polysaccharide capsule that is critical for virulence. Biogenesis of both cell wall and capsule relies on the secretory pathway. Protein secretion begins with polypeptide translocation across the endoplasmic reticulum (ER) membrane through a highly conserved channel formed by three proteins: Sec61, Sbh1, and Sss1. Sbh1, the most divergent, contains multiple phosphorylation sites, which may allow it to regulate entry into the secretory pathway in a species- and protein-specific manner. Absence of *SBH1* causes a cell-wall defect in both *Saccharomyces cerevisiae* and *C. neoformans*, although other phenotypes differ. Proteomic analysis revealed a set of secretory and transmembrane proteins whose expression under host-like conditions was upregulated in wild-type cryptococci, but not in Δ*sbh1* mutant cells. The Sbh1-dependent proteins show specific features of their ER targeting sequences that likely cause them to transit less efficiently into the secretory pathway. Many also act in cell-wall biogenesis, while several are known virulence factors; accordingly, the *C. neoformans* Δ*sbh1* mutant was avirulent in a mouse infection model. We conclude that, in the context of host-like conditions, Sbh1 controls the entry of virulence factors into the secretory pathway of *Cryptococcus neoformans*, and thereby regulates fungal pathogenicity.

Take aways

- *SBH1* is essential for virulence of *C. neoformans*
- Sbh1 is required for increased expression of specific secretory and transmembrane proteins in infection-like conditions
- Sbh1-dependent ER-targeting sequences are suboptimal for entry into the secretory pathway through the Sec61 channel

70 # 1 INTRODUCTION

71 *Cryptococcus neoformans* is a haploid budding yeast that is ubiquitous in the environment, so
72 that spores or dessicated cells are frequently inhaled (Kwon-Chung et al., 2014; Srikanta et
73 al., 2014). In healthy individuals these infectious particles are generally cleared or establish an
74 asymptomatic latent infection (Montoya et al., 2021). If, however, the host is or becomes
75 severely immunocompromised, the pathogen may grow and disseminate, both within and
76 outside of host cells (Gaylord et al., 2020). Dissemination to the central nervous system
77 results in a devastating meningitis, which causes almost 200,000 deaths each year worldwide
78 (Rajasingham et al., 2017).
79
80 Like other fungi, *C. neoformans* is protected by a multilayer cell wall, which is
81 composed of a meshwork of chitin, chitosan, alpha and beta glucans, and mannoproteins
82 (Loza et al., 2021). This flexible and dynamic structure responds to and protects the cell from
83 environmental stresses, while accommodating morphogenesis. An additional role of the
84 cryptococcal wall is to anchor an elaborate polysaccharide capsule that surrounds the cell
85 (Reese et al., 2003; 2007). This structure, which is unique among fungal pathogens, is
86 required for cryptococcal virulence (Kwon-Chung et al., 2014). Capsule polysaccharides are
87 also shed from the cell into the surrounding environment, where they act to perturb the host
88 immune response (Agustinho et al., 2018; Wang et al., 2018).
89
90 The biogenesis of both cell wall and capsule in *C. neoformans* relies on the secretory
91 pathway, which begins with protein translocation across the ER membrane through the highly
92 conserved Sec61 channel (Voorhees & Hegde, 2016). An N-terminal hydrophobic signal
93 peptide or a transmembrane domain targets proteins to this channel, which is formed by three

94 proteins: Sec61, Sbh1, and Sss1 in yeast (Fig. 1A) and Sec61α, Sec61ß, and Sec61γ in
95 mammals (Voorhees & Hegde, 2016; Wu et al., 2019). *SEC61* and *SSS1* are essential in *S.*
96 *cerevisiae* (Stirling et al., 1992; Esnault et al., 1993). The 10 transmembrane helices of Sec61
97 form a protein-conducting channel in the ER membrane, stabilized by Sss1 which clamps
98 around the Sec61 helix-bundle (Fig. 1A) (Wu et al., 2019; Esnault et al., 1994; Falcone et al.,
99 2011). *SBH1* and its paralog *SBH2* are not essential, but deletion of both genes leads to
100 temperature-sensitivity at 37°C in *S. cerevisiae* (Toikkanen et al., 1996; Feng et al., 2007).
101 Sbh1/Sec61ß is a tail-anchored protein associated peripherally with the Sec61 channel
102 (Leznicki et al., 2011) (Fig. 1A). Its conserved transmembrane domain is sufficient to rescue
103 the double mutant growth defect at 37°C, while the role of its divergent cytosolic domain
104 containing multiple phosphorylation sites is poorly understood (Feng et al., 2007; Leroux et
105 al., 2008; Soromani et al., 2012). As is common for proteins with intrinsically unstructured
106 domains, Sbh1/Sec61ß has multiple interactors: it binds to ribosomes and mediates association
107 of the Sec61 channel with signal peptidase and signal recognition particle receptor (Levy et al.,
108 2001; Kalies et al., 1998; Antonin et al., 2000; Jiang et al., 2008). In mammalian cells, the
109 Sbh1 homolog Sec61ß also interacts with the Stimulator of Interferon Genes (STING); this
110 interaction is required for STING's ability to stimulate interferon expression, thus linking the
111 Sec61 channel to the innate immune response (Ishikawa & Barber, 2005). Sec61 with Sss1 can
112 translocate proteins into the ER on its own, but the cytosolic domain of Sec61ß contacts
113 secretory proteins prior to insertion in the cytosolic vestibule of the Sec61 channel and the
114 presence of Sec61ß stimulates import (Kalies et al., 1998; Laird and High, 1997; Besemer et
115 al., 2008). Recently, null mutations in human SEC61B were identified as a cause for
116 polycystic liver disease (Besse et al., 2017). The mutations led to a complete biogenesis defect
117 specific for polycystin-1, a large complex transmembrane protein with a weak secretory signal
118 sequence (Besse et al., 2017). Collectively, these data have led to the view that Sbh1/Sec61ß

119 mediates interaction of the Sec61 channel with other proteins in the ER membrane and that its
120 cytosolic domain aids insertion of specific signal peptides or transmembrane domains into the
121 Sec61 channel.
122
123 Phosphorylation is a frequent biological mechanism for regulation of protein activity or
124 protein-protein interactions and a systematic analysis identifed 63 kinases that play a role in
125 the pathogenicity of *C. neoformans* (Ubersax and Ferrell, 2007; Lee et al., 2016). One of these,
126 Protein Kinase A (PKA), regulates the secretion of a subset of virulence factors (Geddes et al.,
127 2015). Regulation of protein secretion may be important during physiological transitions such
128 as cell differentiation or development. Indeed Sec61ß - the only subunit of the Sec61 channel
129 that has been found to be phosphorylated so far - is important for polarization of epithelial
130 cells, and for development of Drosophila melanogaster embryos (Gruss et al., 1999; Choi et
131 al., 2012; Washiyama et al., 2014; Valcarcel et al., 1999). Both mammalian Sec61ß and yeast
132 Sbh1 are phosphorylated at multiple sites in various combinations (Gruss et al., 1999;
133 Soromani et al., 2012; phosphosite databases). The phosphorylation sites all lie in the
134 intrinsically unstructured cytosolic domain, and are not positionally conserved, with one
135 exception: the proline-flanked site at T5 in *S. cerevisiae* is present in mammals and some
136 birds, although not in lower vertebrates, invertebrates, or other non-pathogenic yeast species.
137 This suggests that this phosphorylation site evolved at least twice by convergent evolution and
138 thus likely has an important function (Fig. 1A, asterisk Fig. 1B) (Soromani et al., 2012).
139
140 The 63 kinases required for virulence of *C. neoformans* include many proline-directed
141 kinases (Lee et al., 2016; Kannan & Neuwald, 2004). When we aligned the N-termini of Sbh1
142 proteins from non-pathogenic and pathogenic yeast, we noticed that - with the exception of
143 *Candida albicans* - all pathogen Sbh1 proteins contain one or more potential proline-flanked

144 phosphorylation site(s) in the N-terminal cytosolic domain, whereas Sbh1 proteins from non-
145 pathogenic yeast species (*Schizosaccharomyces pombe, Kluyveromyces lactis, Yarrowia*
146 *lipolytica, Pichia pastoris, Hansenula polymorpha*) and the *S. cerevisiae* homolog Sbh2 did
147 not (Fig. 1B, pink). This led us to hypothesize that these phosphorylation sites in Sbh1 might
148 be connected to virulence of the respective pathogenic species. In *C. neoformans* Sbh1 the
149 proline-flanked phosphorylation sites are preceded by a potential PKA phosphorylation site
150 (Fig. 1B, blue) and secretion of a subset of virulence factors in *C. neoformans* depends on
151 PKA (Geddes et al., 2015). We therefore decided to investigate the role of Sbh1 and its N-
152 terminal phosphorylation sites in virulence of *C. neoformans*.
153
154 We found that, unlike in *S. cerevisiae,* mutations of the N-terminal Sbh1
155 phosphorylation sites (individually or in combination) do not affect *C. neoformans* growth in
156 rich medium (YPD), and that even complete deletion of *SBH1* only inhibits growth when
157 combined with high temperature and or cell wall stressors. We also observed that in infection-
158 like conditions the deletion mutant fails to properly regulate protein secretion; we have
159 identified the Sbh1-dependent substrates and identified common characteristics of their ER-
160 targeting sequences. Notably, the affected proteins include multiple virulence factors and the
161 mutant is consequently avirulent in a mouse model of infection. Together, our results show
162 that Sbh1 is critical for secretion of a subset of virulence factors and other proteins during *C.*
163 *neoformans* infection, and is therefore essential for its pathogenicity.
164
165

166 # 2 RESULTS

167 ## 2.1 Sbh1 is required for cell wall integrity in *S. cerevisiae* and *C.*
168 *neoformans*

169 We first looked to the best characterized system, *S. cerevisiae*. In this organism, both genes
170 that encode the Sec61 channel beta subunit (*SBH1* and *SBH2*) are required for growth on YPD
171 at 37°C (Fig. 1C) (Toikkanen et al., 1996; Feng et al., 2007; Soromani et al., 2012). In
172 addition, we found that *S. cerevisiae* lacking *SBH1* and *SBH2* have a cell wall defect resulting
173 in resistance to calcofluor white (Fig. 1D, left), indicating reduced chitin in the cell wall, and
174 increased extractability of proteins from the cell wall by alkaline buffer containing
175 dithiotreitol, suggesting structural defects in the cell wall (Fig. 1D, right). While mutation of
176 the conserved Sbh1 phosphorylation site T5 to A on its own has no effect on *S. cerevisiae*
177 growth or cell wall integrity, mutation of both proline-flanked phophorylation sites to A
178 phenocopied the absence of Sbh1 in *S. cerevisiae*. Mutation of both residues to
179 phosphomimetic E had no effect (Fig. 1D).
180
181 The phenotypes we observed in *C. neoformans* cells lacking their sole *SBH1* gene were
182 quite distinct from those of *S. cerevisiae*. Specifically, they showed only modest temperature
183 sensitivity at 37°C on YPD (Fig. 2A, left panel) and no sensitivity to osmotic or cell wall
184 stressors at 30°C (Fig. 2A). At 37°C, however, the mutant cells were hypersensitive to SDS
185 and unable to grow on calcofluor white (Fig. 2B, top two rows); they were also more sensitive
186 than wild-type cells to cell wall digestion by lysing enzymes (Fig. 2C). Of relevance to
187 virulence, the mutant also showed increased sensitivity to oxidative stress (0.1 mM H_2O_2; Fig.
188 2D, top two rows), which is encountered in the setting of infection. Overall, we conclude that
189 Sbh1 is required for cell wall integrity in both the ascomycete *S. cerevisiae* and the

190 basidiomycete *C. neoformans*, although specific manifestations of this requirement differ (see
191 Discussion).
192

193 2.2 Sbh1 N-terminal phosphorylation sites do not affect cell wall
194 integrity in *C. neoformans*

195 As discussed above, we hypothesized that the N-terminal phosphorylation sites in
196 cryptococcal Sbh1 were important for protein function. To test this, we first engineered a
197 plasmid to express wildtype *SBH1* modified with a C-terminal HA tag. The tagged protein
198 effectively complemented the sensitivity of *sbh1*Δ mutants to cell wall stressors (CFW and
199 SDS, Figure 2B). We then modified the expression plasmid such that it would encode Sbh1
200 that was altered to eliminate either the putative PKA site (Ser8 to Ala), two proline-flanked
201 phosphorylation sites (Ser9 to Ala and Thr12 to Val), or all three sites. All of these
202 polypeptides were expressed at similar levels, except for the version with a sole PKA site
203 mutation, which was slightly less abundant (Supplementary Figure 1). We next tested the
204 ability of each construct to complement the growth of *sbh1*Δ cells when challenged with cell
205 wall stressors. Interestingly, each of the modified proteins was as functional as wildtype under
206 these conditions (Fig. 2B). Each of the engineered strains also completely complemented the
207 defective growth of the *sbh1*Δ mutant in the presence of oxidative and nitrosative stress (Fig.
208 2D). These results suggest that, surprisingly, these phosphorylation sites are not required for
209 Sbh1 protein function in *C. neoformans* under the conditions tested.
210

211 2.3 Sbh1-dependent secretory and transmembrane proteins are
212 induced in host-like conditions

213 Sbh1 contacts signal peptides in the cytosolic vestibule of the Sec61 channel, so it can both
214 guide secretory proteins into the channel and control their access to the secretory pathway. To
215 address whether biogenesis of specific secretory or transmembrane proteins was compromised
216 in the absence of *C. neoformans* Sbh1, we grew wild-type and *sbh1*Δ cells in either YPD at
217 30°C or DMEM at 37°C and 5% CO_2 (host-like conditions) and analyzed the proteomes of
218 both strains. We detected no significant differences between wildtype KN99 and *sbh1*Δ strains
219 in YPD at 30°C (Fig. 3), suggesting no critical role for Sbh1 in those conditions. Under host-
220 like conditions, however, we discovered a set of proteins that was specifically induced in wild-
221 type cells, but not in the *sbh1*Δ mutant (Fig. 3, Supplementary Table 1). This set included 32
222 proteins without secretory pathway targeting sequences, 21 transmembrane (TM) proteins and
223 68 proteins with signal peptides (SP) or uncleaved signal anchors (SA) (Supplementary Table
224 1). When we analyzed their ER-targeting sequences we found that the transmembrane domains
225 were slightly more hydrophobic than average for proteins in *C. neoformans*; many also had a
226 strong positively charged patch in close proximity to one side of the TM domain (Fig. 4A;
227 Supplementary Table 2). Some of the transmembrane domains of the Sbh-dependently induced
228 proteins also contained a high number of prolines and/or glycines in addition to the polybasic
229 stretch adjacent to the transmembrane domain (Supplementary Table 2). The Sbh1-dependent
230 signal peptides were more heterogeneous, but most displayed reduced C-region polarity (Fig.
231 4B; Supplementary Table 2). In addition, they were suboptimal in various ways which
232 therefore defied bioinformatic analysis: some had limited hydrophobicity, some contained
233 high numbers of proline and glycine which interfere with alpha-helix formation, and many had
234 a charge bias problem (either no charge on either side of the hydrophobic core, or a positive
235 charge C-terminal instead of N-terminal of the hydrophobic core, or multiple positive charges
236 at the N-terminus of the mature part of the protein) (Supplementary Table 2). Because signal

237 peptides insert as alpha-helices into the hydrophobic lateral gate of the Sec61 channel with the
238 positively charged N-terminus towards the cytosol, any of these features will reduce
239 translocation efficiency into the ER. We conclude that Sbh1 is required for the biogenesis of
240 specific secretory and transmembrane proteins under host-like conditions. Because the
241 targeting sequences of these proteins are suboptimal for Sec61 channel insertion, they rely on
242 the enhanced insertion efficiency provided by the presence of Sbh1 (Fig. 4C) (Kalies et al.,
243 1998).
244

245 2.4 Sbh1 is essential for virulence of *C. neoformans*

246 The proteome analysis presented above shows that Sbh1 regulates the secretion of proteins
247 that are induced by a host-like environment. This process is likely important for pathogenesis,
248 as supported by our observation that *sbh1*Δ cells have a reduced ability to survive within host
249 macrophages (Supplementary Figure 2). To directly test the role of Sbh1 in virulence, we used
250 a well-established mouse model for cryptococcal infection. At 14 days after intransal infection
251 we observed a striking reduction in both lung and brain fungal burden in *sbh1*Δ-infected
252 animals compared to wild type (Figure 5). Consistent with this finding, mice infected with
253 wild-type cryptococci succumbed to infection within 18 days, while mutant-infected animals
254 remained healthy and grew normally for at least 10 weeks (Figure 5 and Supplementary Figure
255 3). We conclude that *SBH1* is essential for *Cryptococcus neoformans* virulence.

256 # 3 DISCUSSION

257 In this work we sought to identify factors regulating secretion of virulence-relevant proteins in
258 the human pathogen *C. neoformans*. We specifically investigated the role of the non-essential
259 ER protein translocation channel subunit Sbh1. Since the Sbh1 cytosolic domain contacts
260 secretory signal sequences in the cytosolic vestibule of the channel prior to insertion into the
261 channel it can potentially aid or restrict protein import into the secretory pathway of specific
262 proteins under specific growth conditions. This may be regulated by phosphorylation as Sbh1
263 in all species contains multiple phosphorylation sites which are only partially positionally
264 conserved (Fig. 1A, B).
265
266 In *S. cerevisiae*, absence of *SBH1* and its paralog *SBH2* causes temperature sensitivity
267 (Fig. 1C; Finke et al., 1996; Feng et al., 2007). The reason for this is still unclear, as ER
268 translocation defects at the restrictive temperature are modest for most substrates investigated
269 (Finke et al., 1996; Feng et al., 2007). We show here that *S. cerevisiae* Sbh1 is important for
270 cell wall integrity, and that cell wall integrity specifically requires the two proline-flanked N-
271 terminal phosphorylation sites at S3 and T5 (Fig. 1D). Proline-flanked phosphorylation sites in
272 Sbh1 of other yeast species occur primarily in human pathogens (Fig. 1B), which suggested to
273 us that phosphorylation at these sites may play a regulatory role in virulence. The absence of
274 *SBH1* in *C. neoformans* resulted only in a very modest temperature sensitivity at 37°C (Fig.
275 1C vs. 2A), although at high temperature *sbh1*Δ *C. neoformans* also displayed a cell wall
276 defect (Fig. 2A-C). In contrast to *S. cerevisiae*, however, mutation of the N-terminal proline-
277 flanked phosphorylation sites of *C. neoformans* Sbh1 individually or in combination did not
278 phenocopy the cell wall defect (Fig. 2B). As protein kinase A has been shown to be critical for
279 *C. neoformans* virulence, and Sbh1 also contains a PKA site in *C. neoformans* (Fig. 1B, blue),
280 we also mutated this site alone or in combination with the proline-flanked sites, but again saw

281 no effect on cell wall integrity (Fig. 2B) (Geddes et al., 2015). Taken together, our data
282 suggest that Sbh1 is important for efficient secretion of one or more enzymes or precursors for
283 the cell wall in both *S. cerevisiae* and in *C. neoformans*, but that the role of the N-terminal
284 proline-flanked phosphorylation sites in this process is different in the two organisms.
285 Alternatively, the differential effect of the phosphorylation site mutations may reflect
286 differences in the cell wall compositions: whereas the *S. cerevisiae* cell wall is formed by ß-
287 1,3-glucan, ß-1,6-glucan, chitin, and mannoproteins, in the *C. neoformans* cell wall most
288 chitin is deacylated to chitosan, and α-1,3-glucan is a major cell wall component (Lessage and
289 Bussey, 2006; Wang et al., 2018).
290
291 We next asked which proteins were affected by absence of *SBH1* in *C. neoformans*.
292 Using a proteomic approach we identified a set of secretory and transmembrane proteins that
293 were induced under infection-like conditions (DMEM at 37°C and 5%CO_2) in the wild-type
294 strain, but not in the *sbh1*Δ mutant (Fig. 3; Supplementary Tables S1 and S2). Many of the
295 membrane proteins in this set were characterized by a strong polybasic patch adjacent to the
296 first transmembrane domain (e.g. CNAG_1854, CNAG_5502, CNAG_6416), while the signal
297 peptides of the secretory proteins were more heterogeneous, and had less polar C-regions than
298 average (Supplementary Table S2; Fig. 4A, B). This is reminiscent of the ER targeting signals
299 identified by Ziska and colleagues in mammalian cells whose ER import was dependent on the
300 Sec61 channel-interacting protein Sec63 and the ER-lumenal Hsp70 chaperone BiP (Ziska et
301 al., 2019). In *S. cerevisiae* the Sec63 complex composed of Sec63, Sec62, Sec71, and Sec72
302 promotes posttranslational protein import into the ER through the Sec61 channel by stabilizing
303 the lateral gate in a partially open conformation (Itskanov and Park, 2019; Wu et al., 2019). It
304 also plays a role in membrane protein topogenesis in both yeast and mammalian cells (Mades
305 et al., 2012; Jung et al., 2014). Sec63 is a polytopic membrane protein with an ER-lumenal J-

306 domain that activates ATP-hydrolysis of the ER-lumenal chaperone BiP (Kar2 in yeast)
307 (Vembar et al., 2010). Kar2 contributes to protein import into the ER either by directly binding
308 to the incoming protein or by promoting its folding (Matlack et al., 1999; Allen et al., 2019).
309 As proteins dependent on Sbh1 in *C. neoformans* and proteins dependent on Sec63/BiP in
310 mammalian cells have similar characteristics, our data suggest that Sbh1 and the Sec63
311 complex have overlapping functions in promoting ER import of specific proteins.
312
313 Signal peptides generally insert into the Sec61 channel with their N-terminus towards
314 the cytosol and their N-terminal positive charge (Fig 4B, '+') contributes to this orientation
315 (Hegde and Bernstein, 2006). Many of the Sbh1-dependent signal peptides we identified in *C.*
316 *neoformans* have no charge bias towards the N-terminus; in some, the charge bias is even
317 reversed (Supp. Table S2). Sbh1 may help orient such signal peptides in the cytosolic
318 vestibule of the Sec61 channel with the help of its cytosolic domain. The polar C-region of
319 signal peptides contains the signal peptidase cleavage site (Hegde and Bernstein, 2006). Most
320 of the Sbh1-dependent signal peptides we identified have a very short C-region (Supp. Table
321 S2) which may limit signal peptidase access unless the signal peptide is positioned accurately
322 by Sbh1. In order to efficiently insert into the Sec61 channel the signal peptides of secretory
323 proteins require an alpha-helical hydrophobic region (Fig 4B, H region, blue) (Hegde and
324 Bernstein, 2006). Many of the Sbh1-dependent signal peptides of *C. neoformans* contain
325 multiple helix-breaking P or G residues within their hydrophobic helical core regions, and
326 some have very short or very long hydrophobic H-regions (Supp. Table 2). These features
327 would make it difficult for signal peptides to stably insert into the Sec61 channel lateral gate.
328 Overexpression of an N-terminally truncated Sbh1 lacking most of its cytosolic domain
329 complements the temperature-sensitivity and at least some of the translocation defect in Δ*sbh1*
330 Δ*sbh2 S. cerevisae* (Feng et al., 2007). Together with our data, this suggests that the Sbh1

331 transmembrane domain stabilizes a conformation of the Sec61 lateral gate that favours
332 insertion of the helical hydrophobic core of signal peptides, even if they are suboptimal.
333
334 That Sbh1-dependent secretion is critical for virulence is illustrated by both the
335 reduced intracellular fitness of *sbh1*Δ *C. neoformans* in macrophages and the effects in mice:
336 in contrast to infection with KN99 wildtype *C. neoformans* which resulted in a high burden in
337 the lungs and death of all mice by day 18 post infection, all mice infected with *sbh1*Δ *C.*
338 *neoformans* survived for 70 days and even gained weight (Supp Fig 3), indicating that the
339 mutant strain was avirulent.
340
341 We hypothesize that the striking defect in virulence of the *sbh1* mutant reflects
342 reduced secretion of multiple groups of proteins. For a few examples, these could include
343 proteins required for fungal growth in the host environment (e.g. metabolic genes or proteins
344 involved in cell wall synthesis), needed for virulence factor production, or directly involved in
345 host damage. To explore this idea, we reviewed the polypeptides whose secretion is most
346 impaired in the absence of Sbh1 (Supplementary Table 1), focusing on proteins with signal or
347 transmembrane sequences that had been previously implicated in cryptococcal virulence. We
348 identified eight such proteins, which had exhibited infectivity defects in a large-scale screen
349 (Liu et al., 2008) and/or been individually studied and shown to contribute to virulence (Table
350 1). Two proteins in this group (Pbx1(Liu et al., 2007; Kumar et al., 2014) and Skn1 (Gilbert
351 et al., 2010)) act in cell wall synthesis, so their reduced secretion could contribute to the wall
352 defects and sensitivity to host-induced stress that we observed in *sbh1* mutant cells. Another
353 is required for capsule display (Cap60 (Chang et al., 2998)), although its biochemical function
354 has not been characterized, and two others are proteases (CNAG_00150 and Mpr1 (Vu et al.,
355 2014)). Many fungal proteases damage host tissues during infection (Monod et al., 2002) and

356 Mpr1 further acts in cryptococcal crossing of the blood-brain barrier (Vu et al., 2014), which
357 is required for cryptococcal dissemination to the brain and subsequent lethality. Supporting a
358 role in infection for this group of proteins, six of the corresponding genes are expressed more
359 highly in host-like conditions than in rich medium (one other is modestly decreased); this
360 pattern is particularly striking for *CIG1* and *MPR1*, whose expression levels increase over
361 100-fold (Table 1) (Maier et al., 2015). Notably, the evidence that these proteins are
362 important for cryptococcal virulence derives from studies of individual gene deletion strains,
363 which completely lack one of these target proteins. The situation in the *sbh1* mutant is
364 different, in that many proteins are secreted less efficiently, but none (besides Sbh1) are
365 absent. Nonetheless, the impaired secretion of multiple proteins with key roles in virulence,
366 together with others in the functional groups above, provides abundant reason for the inability
367 of *sbh1* to cause disease in a mammalian host.

368

369 We conclude that *C. neoformans* Sbh1 is important for biogenesis of virulence factors
370 whose specific ER-targeting sequences make these proteins dependent on Sbh1 for ER import
371 (Fig. 4C). Recently, Sec61beta has also been shown to be critical for infection by the
372 important fungal crop pathogen *Magnaporthe oryzae*, suggesting a more general role for
373 Sbh1/Sec61beta in fungal infection (Wei et al., 2020). Since the intrinsically unstructured N-
374 terminal part of the Sbh1 cytosolic domain is not conserved between yeast and mammals, *C.*
375 *neoformans* Sbh1 may serve as a new specific target for developing drugs against this
376 important human pathogen.

377

378 # 4 EXPERIMENTAL PROCEDURES

379 ## 4.1. *S. cerevisiae* strains and growth conditions

380 NY179 (*SBH1 SBH2 MAT* a *leu2-3,112 ura3-52*), H3223 (MAT a *KanMx::sbh1 leu2-3,112*
381 *ura3-52 GAL*$^{+}$), H3203 (MAT a *HphMx::sbh2 leu2-3,112 ura3-52 GAL*$^{+}$), and H3231 (MAT
382 a *KanMx::sbh1 HphMx::sbh2 leu2-3,112 ura3-52 GAL*$^{+}$) were gifts from Jussi Jäntti and used
383 to characterize Sbh1p phosphorylation sites (Toikkanen et al., 1996; Feng et al., 2007). *SBH1*
384 cloned into pCR2.1-TOPO plasmid was kindly provided by Jussi Jäntti (Helsinki University,
385 Finland). The QuickChange Site-Directed Mutagenesis Kit (Stratagene, UK) was used to
386 introduce single or multiple base mutations in *SBH1.* Substitutions were verified by
387 sequencing. Mutated *sbh1* was excised from pCR2.1-TOPO plasmids using EcoRV/BamHI,
388 and subcloned into pRS415. For growth assays cells were grown on YPD or synthetic
389 complete medium without leucine and with or without 10 µg/ml calcofluor white (Sigma) at
390 30°C or 37°C for 3 days.
391

392 ## 4.2 *S. cerevisiae* cell wall extraction

393 Cells were grown in synthetic complete medium without leucine to early exponential phase
394 and 10 OD_{600} harvested by centrifugation. Cells were resuspended in 100 µl 100 mM Tris-
395 HCl, pH 9.4, 10 mM DTT, and incubated for 15 min at 37°C shaking at 800 rpm in a
396 Thermomixer (Eppendorf). Samples were chilled for 1 min on ice, followed by sedimentation
397 of the cells in a refrigerated Eppendorf centrifuge at maximal speed for 1 min. 90 µl of each
398 supernatant were transferred to a new tube, carefully avoiding the pellet, and centrifuged again
399 as above. 80 µl of each supernatant were transferred to a fresh tube and proteins precipitated
400 by adding an equal volume of ice-cold 20 % trichloroacetic acid. Samples were mixed
401 thoroughly and incubated on ice for 30 min. Proteins were sedimented by centrifugation at

402 4°C for 15 min and the pellets washed with ice-cold acetone, dried, and resuspended in 20 µl
403 2x SDS sample buffer by heating for 10 min to 95°C with agitation. Proteins were resolved on
404 4-14% Bis-Tris gels (NuPage) run in MOPS buffer and revealed by Coomassie staining.
405

406 4.3 *C. neoformans* strains and growth conditions

407 All strains used were in the *C. neoformans* serotype A strain KN99α background. The
408 *sbh1*Δ deletion in this background used here was obtained from a library of partial gene
409 deletions (generated by the Madhani group (Liu et al, 2008) and available from the Fungal
410 Genetics Stock Center at Kansas State University, Manhattan, KS) and confirmed by PCR.
411 Fungal stocks were maintained at -80°C and grown at 30°C on yeast peptone dextrose
412 (YPD) media with antibiotics as appropriate (100 µg/mL of nourseothricin (clonNAT,
413 WERNER BioAgents, Germany) or 100 µg/mL G418 (Geneticin, Life Technologies,
414 USA)).
415

416 4.4 *SBH1* plasmid construction

417 For plasmid construction, the *SBH1* gene with its promoter and terminator sequences was
418 amplified and cloned into ApaI/SpeI-digested pIBB103 (Skowyra and Doering, 2012). In
419 parallel, a similar fragment lacking the terminator sequences and stop codon was amplified
420 and cloned into ApaI/SpeI-digested pFS5XHA (pIBB103 containing 5 HA epitopes followed
421 by the *TRP1* terminator; this study). After both versions were confirmed to complement
422 phenotypic defects, the tagged version was used for all subsequent analyses. This construct
423 was used as template for mutagenesis of the N-terminal motifs of *SBH1* by using overlapping
424 primers containing the codon changes and the forward and reverse primers used above. The
425 resulting product was digested, cloned into pFS5XHA, and the whole insert sequenced to

426 confirm mutations. These plasmids, together with an empty plasmid control, were
427 electroporated into KN99α and the *sbh1*Δ strains as detailed below.
428

429 4.5 Electroporation of *C. neoformans*

430 Plasmid transformation was done by electroporation as described in (Skowyra and Doering,
431 2012). In brief, *Cryptococcus* cells patched on YPD agar plates with appropriate antibiotics
432 were transferred into 5 ml of YPD liquid medium with antibiotic and cells were grown
433 overnight at 30°C with shaking at 250 rpm. The overnight culture was diluted to an OD_{600} of
434 0.05 in 50 ml of fresh YPD medium (note that this OD_{600} value was measured in a multiplate
435 reader and was not corrected for pathlength). After two doubling times the cells were
436 transferred into conical tubes and sedimented, washed twice with cold dH_2O, and resuspended
437 thoroughly in 50 ml cold EB buffer (10 mM Tris-HCl, pH 7.5, 1 mM $MgCl_2$, and 270 mM
438 Sucrose) with 4 mM DTT. After incubation on ice for 15 min, the cells were pelleted, washed
439 with 50 ml EB buffer without DTT, and resuspended in 1 ml EB buffer for counting. Cells
440 were adjusted to 300 million cells per 100 µl, mixed with at least 1 µg of DNA (in no more
441 than 1/10 of the total volume) and the mixture transferred into ice-cold 2 mm gap cuvettes. A
442 Biorad electroporator was used with the following settings: V = 500v, R = infinity ohms, C =
443 25µF; the time constant should be 15 – 25 ms. Immediately after electroporation, 900 µl YPD
444 without antibiotics was added and the cell suspension was transferred to a culture tube and
445 incubated at 30°C for 3-4 h for recovery before various dilutions were spread on YPD plates
446 with antibiotics to select transformants. Because of the heterogeneity in copy number
447 associated with plasmids in *C. neoformans*, at least three independent colonies were picked
448 and tested for each construct. All exhibited the same behaviors.
449
450

451 ## 4.6 Dot spotting on stress plates

452 Strains to be tested were grown overnight in YPD with antibiotic, diluted to an OD_{600} of 0.05
453 in fresh YPD, and grown for two doublings. The cultures were then adjusted to 2 x 10^9
454 cells/ml, serially diluted (10-fold) and 5 µl aliquots were spotted onto the phenotyping plates
455 described in the text. These plates did not include antibiotics because in combination with
456 stressors they inhibit cell growth. Plates were incubated at 30°C and 37°C for 3-4 days.
457

458 ## 4.7 Sensitivity to lysing enzyme

459 The assay for sensitivity to lysing enzymes was adapted from (Gerik et al., 2005). Briefly,
460 overnight cultures of wild type and mutant strains in YPD medium were washed once with
461 PBS and once with citrate buffer (10 mM, pH 6.0). Cells were resuspended in citrate buffer
462 and the OD_{600} was normalized to 1.0/ml with the same buffer. 1 ml aliquots were then
463 subjected to centrifugation and the pellets (one per time point) were resuspended in a solution
464 of lysing enzyme (final concentration 25 mg/ml; Sigma, L-1412) and incubated at 37°C with
465 gentle agitation. At each desired timepoint one aliquot per strain was sedimented and
466 resuspended in the same volume of distilled water (in the absence of lysis the OD_{600} should
467 remain ~1.0). The assay was performed independently three times.
468

469 ## 4.8 Mass spectrometry analysis

470 For total cellular proteome analysis, cells were collected by centrifugation at 3,500 rpm for 10
471 min and the pellets were washed twice with cold PBS before being subjected to acetone
472 precipitation and enzymatic digestion (Geddes et al., 2016; Ball and Geddes-McAlister,
473 2019). For secretome analysis, supernatant fractions from *C. neoformans* WT and *sbh1*Δ cell
474 cultures were collected and filtered using 0.22 µM syringe filters and subjected to in-solution

475 trypsin digestion (Ball and Geddes-McAlister, 2019). Digestion was stopped by the addition
476 of 10% v/v trifluoroacetic acid (TFA) and the acidified peptides were desalted and purified
477 according to the standard protocol (Rappsilber et al., 2007). Approximately 50 µg of sample
478 was loaded onto StageTips and stored at 4°C until LC-MS/MS measurement.
479
480 For LC-MS/MS measurement, samples were analyzed by nanoflow liquid
481 chromatography on an EASY-nLC 1200 system (ThermoFisher Scientific) on-line coupled to
482 a Q Exactive HF-X quadrupole orbitrap mass spectrometer (ThermoFisher Scientific). An in-
483 line 75 µm x 50 cm PepMap RSLC EASY-Spray column filled with 2 µm C18 beads
484 (ThermoFisher Scientific) separated peptides using linear gradients from 3% to 20% Buffer B
485 (80% acetonitrile) over 18 min and from 20% to 35% Buffer B over 31 minutes, followed by
486 a steep 2 min ramp to 100% Buffer B for 9 min in 0.1% Formic acid at a constant flow
487 of 250 nl/min.
488
489 Raw files were analyzed together using MaxQuant software (version 1.6.0.26) (Cox &
490 Mann, 2008). The derived peak list was searched with the built-in Andromeda search engine
491 (Cox et al., 2011) against the reference *C. neoformans* H99 proteome downloaded from
492 Uniprot (http://www.uniprot.org/) (Aug. 18, 2018; 7,430 sequences). The mass spectrometry
493 proteomics data have been deposited in the PRIDE partner repository for the
494 ProteomeXchange Consortium with the data set identifier: PXD013894.
495
496 Statistical analysis of the MaxQuant-processed data was performed using the
497 Perseus software environment (version 1.6.2.2) (Tyanova et al., 2016). A Student's *t*-
498 test was performed to identify proteins with a significant differential expression (*p-value* <
499 0.05) (S_0 = 1) between samples employing a 5% permutation-based FDR filter.

500 ## 4.9 In vitro macrophage survival assay

501 Fungal survival after engulfment by THP-1 (ATCC #TIB-202) cells *in vitro* was assessed as
502 in (Santiago-Tirado et al., 2015) with only minor modifications: First, since the cryptococcal
503 strains were grown in G418 for plasmid maintenance, they were washed extensively with
504 PBS to remove all traces of drug before being opsonized, adjusted to an MOI of 10, and
505 added to the THP-1 cells. Second, for CFU determination, 0.1% Triton-X100 (which had no
506 effect on the cryptococcal cells) was used instead of SDS to lyse the THP-1 cells.

507

508 ## 4.10 Infection studies

509 Strains to be tested were cultured overnight in YPD medium, collected by centrifugation,
510 washed in PBS, and diluted to 10^6 cells/ml in PBS for intranasal inoculation (50 µl) into 4-6
511 week-old female C57BL/6 mice (National Cancer Institute) that had been anesthetized with a
512 combination of ketaset-HCl and xylazine. Initial inocula were plated to confirm CFUs. To
513 assess long-term survival, infected animals were weighed 1 h post-infection and at least every
514 other day afterwards. Mice were sacrificed if their weight fell below 80% of peak (an outcome
515 which in this protocol precedes any signs of disease) or at the end of the study (10 weeks). To
516 measure organ burden, infected mice were monitored as above for 14 days, at which point lungs
517 and brains were harvested from all mice, homogenized in PBS, and serial dilutions of the
518 homogenate plated on YPD agar for enumeration of CFU.

519

520

521

522

523 ## ETHICS STATEMENT

524 All animal studies were reviewed and approved by the Animal Studies Committee of
525 Washington University School of Medicine and conducted according to the National Institutes
526 of Health guidelines for housing and care of laboratory animals.
527

528 ## CONFLICT OF INTEREST

529 The authors declare no conflict of interest.
530

531 ## ACKNOWLEDGMENTS

532 We thank William Allen, Bristol University, for help with Fig. 1A; Christina Soromani,
533 Andrea Ludes, and Nicole Spitzlberger (all former students of the Römisch lab) for data
534 shown in Fig. 1C; and Jussi Jäntti, VTT Helsinki, for *S. cerevisiae* strains and plasmids.
535

536 ## DATA AVAILABILITY

537 Proteomics .Raw data files are available in the PRIDE (Proteomics Identification Database):
538 Project ID: PXD013894
539 **Username:** reviewer78525@ebi.ac.uk
540 **Password:** 8ZiMfbKG
541

542 ## FUNDING

543 JGM is supported by the Canadian Foundation for Innovation (JELF #38798) and the
544 Canadian Institutes for Health Research (Project Grant). KR is supported by a core grant from
545 the Saarland University. Work in the Doering lab was supported by NIH grants AI140979 and

546 AI135012 to TLD. FHS also received support from NIH T32 grant AI007172 and a
547 Postdoctoral Enrichment Program Award from the Burroughs Wellcome Fund.

548

549 # REFERENCES

550 Agustinho DP, Miller LC, Li LX, and Doering TL (2018). Peeling the onion: the outer layers
551 of *Cryptococcus neoformans*. *Mem Inst Oswaldo Cruz* 113:e180040.
552 Allen WJ, Collinson I, Römisch K (2019). Post-translational protein transport by the Sec
553 complex. Trends Biochem Sci pii:S0968-0004(19)30056-8.
554 Antonin W, Meyer HA, Hartmann E (2000). Interactions between Spc2 and other components
555 of the endoplasmic reticulum translocation sites of the yeast *Saccharomyces cerevisiae*. *J*
556 *Biol Chem* 275:34068-72.
557 Ball B, Geddes-McAlister J (2019). Quantitative Proteomic Profiling of *Cryptococcus*
558 *neoformans*. *Curr Protocols Microbiology* 55:e94.
559 Besemer J, Harant H, Wang S, Oberhauser B, Marquardt K, Foster SA, Schreiner EP, de
560 Vries JE, Dascher-Nadel C, Lindley IJD (2005). Selective inhibition of cotranslational
561 translocation of vascular cell adhesion molecule 1. *Nature* 436:290-93.
562 Besse W, Dong K, Choi J, Punia S, Fedeles SV, Choi M, Gallagher AR, Huang EB, Gulati A,
563 Knight J, ManeS, Tahvanainen E, Tahvanainen P, Sanna-Cherchi S, Lifton RP, Watnick
564 T, Pei YP, Torres VE, Somlo S (2017). Isolated polycystic liver disease genes define
565 effectors of polycystin-1 function. *J Clin Invest* 127:1772-85.
566 Cadieux B, Lian T, Hu G, Wang J, Biondo C, Teti G, Liu V, Murphy M, Creagh, AL, and
567 Kronstad JW (2013). The Mannoprotein Cig1 supports iron acquisition from heme and
568 virulence in the pathogenic fungus *Cryptococcus neoformans*. *J Infect Dis* 207:1339-
569 1347.

570 Chang YC, Kwon-Chung KJ (1998). Isolation of the third capsule-associated gene, *CAP60*,
571 required for virulence in *Cryptococcus neoformans*. *Infect Immun* 66:2230-2236.
572 Choi SY, Fogelgren B, Zuo, Z, Juang L, McKenna S, Lingappa VR, Lipschutz JH (2012).
573 Exocyst Sec10 is involved in basolateral protein translation and translocation in the
574 endoplasmic reticulum. *Nepron Exp Nephrol* 120:e133-e139.
575 Cox J, Mann M (2008). MaxQuant enables high peptide identification rates, individualized
576 ppb-range mass accuracies and proteome-wide quantification. *Nature Biotechnol*
577 26:1367-72.
578 Cox J, Neuhauser N, Michalski A, Scheltema RA, Olsen JV, Mann M (2011). Andromeda: A
579 peptide search engine integrated into the MaxQuant environment. J Proteome Res
580 10:1794-805.
581 Cox J, Hein MY, Luber CA, Paron I, Nagarj N, Mann M (2014). Accurate proteome-wide
582 label-free quantitation by delayed normalization and maximal peptide ratio extraction,
583 termed MaxLFQ. Mol Cell Proteomics 13:2513-26.
584 Esnault Y, Blondel M, Deshaies R, Schekman R, Képès F (1993). The yeast SSS1 gene is
585 essential for secretory protein translocation and encodes a conserved protein of the
586 endoplasmic reticulum. *EMBO J* 12:4083–93.
587 Esnault, Y, Feldheim, D, Blondel, MO, Schekman, R, and Képès, F (1994). *SSS1* encodes a
588 stabilizing component of the Sec61 subcomplex of the yeast protein translocation
589 apparatus. *J Biol Chem* 269:27478–24785.
590 Falcone D, Henderson MP, Nieuwland H, Coughlan CM, Brodsky JL, Andrews DW (2011).
591 Stability and function of the Sec61 translocation complex depends on the Sss1p tail-
592 anchor sequence. *Biochem J* 436:291-303.

593 Feng D, Zhao X, Soromani C, Toikkanen J, Römisch K, Vembar SS, et al (2007). The
594 transmembrane domain is sufficient for Sbh1p function, its association with the Sec61
595 complex, and interaction with Rtn1p. *J Biol Chem* 282:30618-28.
596 Finke K, Plath K, Panzner S, Prehn S, Rapoport TA, Hartmann E, Sommer T (1996). A
597 second trimeric complex containing homologs of the Sec61p complex functions in
598 protein transport across the ER membrane of *S. cerevisiae*. *EMBO J* 15:1482-94.
599 Gaylord EA, Choy HL, and Doering TL (2020). Dangerous Liaisons: Interactions of
600 *Cryptococcus neoformans* with Host Phagocytes. *Pathogens* 9:891-905.
601 Geddes JMH, Croll D, Caza M, Stoynov N, Foster LJ, Kronstad JW (2015). Secretome
602 profiling of *Cryptococcus neoformans* reveals regulation of a subset of virulence-
603 associated proteins and potential biomarkers by protein kinase A. *BMC Microbiology*
604 15:206.
605 Geddes JM, Caza M, Croll D, Stoynov N, Foster LJ, Kronstad JW (2016). Analysis of the
606 protein kinase A-regulated proteome of *C. neoformans* identifies a role for the ubiquitin-
607 proteasome pathway in capsule formation. MBio 7:e01862-15.
608 Gerik KJ, Donlin MJ, Soto CE, Banks AM, Banks IR, Maligie MA, Selitrennikoff CP, Lodge
609 JK (2005). Cell wall integrity is dependent on the *PKC1* signal transduction pathway in
610 *Cryptococcus neoformans*. *Mol Microbiol* 58:393–408.
611 Gilbert NM, Donlin MJ, Gerik KJ, Specht CA, Djordjevic JT, Wilson CF, Sorrell TC, Lodge
612 JK (2010). *KRE* genes are required for beta-1,6-glucan synthesis, maintenance of capsule
613 architecture and cell wall protein anchoring in *Cryptococcus neoformans*. *Mol Microbiol*
614 76:517-534.
615 Gruss OJ, Feick P, Frank R, Dobberstein B (1999). Phosphorylation of components of the ER
616 translocation site. *Eur J Biochem* 260:785-793.

617 Hegde RS, Bernstein HD (2006). The surprising complexity of signal sequences. *Trends*
618 *Biochem Sci* 31:563-571.
619 Itskanov S, Park E (2019). Structure of the posttranslational Sec protein translocation channel
620 complex from yeast. *Science* 363:84-87.
621 Ishikawa H, Barber GN (2005). STING is an endoplasmic reticulum adaptor that facilitates
622 innate immune signalling. *Nature* 455:674-679.
623 Jiang Y, Cheng Z, Mandon EC, Gilmore R (2008). An interaction between the SRP receptor
624 and the translocon is critical during cotranslational protein translocation. *J Cell Biol*
625 180:1149-1161.
626 Jung SJ, Kim JE, Reithinger JH, Kim H (2014). The Sec62-Sec63 translocon facilitates
627 translocation of the C-terminus of membrane proteins. *J Cell Sci* 127:4270-78.
628 Kalies K-U, Rapoport TA, Hartmann E (1998). The β subunit of the Sec61 complex
629 facilitates cotranslational protein transport and interacts with signal peptidase during
630 translocation. *J Cell Biol* 141:887–94.
631 Kannan N, Neuwald AF (2005). Evolutionary constraints associated with functional
632 specificity of the CMGC protein kinases MAPK, CDK, GSK, SRPK, DYRK, and
633 CK2alpha. *Protein Sci* 13:2059-77.
634 Kumar P, Heiss C, Santiago-Tirado FH, Black I, Azadi P, Doering TL (2014). Pbx proteins in
635 *Cryptococcus neoformans* cell wall remodeling and capsule assembly. *Eukaryot Cell*
636 13:560-571.
637 Kwon-Chung K, Fraser, JA, Doering TL, Wang Z, Janbon G, Idnurm A, and Bahn YS (2014).
638 *Cryptococcus neoformans* and *Cryptococcus gattii,* the etiologic agents of
639 cryptococcosis. *Cold Spring Harbor perspectives in medicine* 4:a019760.
640 Laird V, High S (1997). Discrete cross-linking products identified during membrane protein
641 biosynthesis. *J Biol Chem* 272:1983-1989.

642 Lee KT, So YS, Yang DH, Jung KW, Chio J, et al. (2016). Systematic functional anallysis of
643 kinases in the fungal pathogen *Cryptococcus neoformans*. *Nature Communications*
644 7:12766.
645 Lesage G, Bussey H (2006). Cell wall assembly in *Saccharomyces cerevisiae*. Microbiol Mol
646 Biol Reviews 70:317-343.
647 Levy R, Wiedmann M, Kreibich G (2001). *In Vitro* binding of Ribosomes to the ß subunit of
648 the Sec61p protein translocations complex. *J Biol Chem* 276:2340-2346.
649 Leznicki P, Warwicker J, High S (2011). A biochemical analysis of the constraints of tail-
650 anchored protein biogenesis. *Biochem J* 436:719-727.
651 Liu OW, Kelly MJ, Chow ED, Madhani HD (2007). Parallel beta-helix proteins required for
652 accurate capsule polysaccharide synthesis and virulence in the yeast *Cryptococcus*
653 *neoformans*. *Eukaryot Cell* 6:630-640.
654 Liu OW, Chun CD, Chow ED, Chen C, Madhani HD, Noble SM (2008). Systematic genetic
655 analysis of virulence in the fungal pathogen *Cryptococcus neoformans*. Cell 135:174-
656 188.
657 Loza L, and Doering TL (2021). Glycans of the pathogenic yeast *Cryptococcus neoformans*
658 and related opportunities for therapeutic advances. in *Comprehensive Glycoscience*
659 (Barchi, J. ed.), 2nd Ed., Elsevier.
660 Mades A, Gotthardt K, Awe K, Stieler J, Döring T, Füser S, Prange R (2012). Role of human
661 Sec63 in modulating the steady-state levels of multi-spanning membrane proteins. *PLoS*
662 *One* 7:e49243.
663 Maier EJ, Haynes BC, Gish SR, Wang ZA, Skowyra ML, Marulli AL, Doering TL, Brent MR
664 (2015). Model-driven mapping of transcriptional networks reveals the circuitry and
665 dynamics of virulence regulation. *Genome Res* 25: 690-700.

666 Monod M, Capoccia S, Lechenne B, Zaugg C, Holdom M, Jousson O (2002). Secreted
667 proteases from pathogenic fungi. *Int J Med Microbiol* 292:405-419.
668 Montoya MC, Magwene PM, and Perfect JR (2021). Associations between Cryptococcus
669 Genotypes, Phenotypes, and Clinical Parameters of Human Disease: A Review. *J Fungi*
670 *(Basel)* 7: 260.
671 Rajasingham R, Smith RM, Park BJ, Jarvis JN, Govender NP, Chiller TM, Denning DW,
672 Loyse A, and Boulware DR (2017). Global burden of disease of HIV-associated
673 cryptococcal meningitis: an updated analysis. *Lancet Infectious Dis* 17:873-881.
674 Rappsilber J, Mann M, Ishihama Y (2007). Protocol for micro-purification, enrichment, pre-
675 fractionation and storage of peptides for proteomics using Stage Tips. Nat Protoc 2:1896-
676 906.
677 Reese AJ, and Doering TL (2003). Cell wall alpha-1,3-glucan is required to anchor the
678 *Cryptococcus neoformans* capsule. *Mol Microbiol* 50:1401-1409.
679 Reese AJ, Yoneda A, Breger JA, Beauvais A, Liu H, Griffith CL, Bose I, Kim MJ, Skau C,
680 Yang S, Sefko JA, Osumi M, Latge JP, Mylonakis E, and Doering TL (2007). Loss of
681 cell wall alpha(1-3) glucan affects *Cryptococcus neoformans* from ultrastructure to
682 virulence. *Mol Microbiol* 63:1385-1398.
683 Santiago-Tirado FH, Peng T, Yang M, Hang HC, Doering TL (2015). A single protein S-acyl
684 transferase acts through diverse substrates to determine cryptococcal morphology, stress
685 tolerance, and pathogenic outcome. *PLoS Pathog* 11(5):e1004908.
686 Skowyra ML, Doering TL (2012). RNA interference in *Cryptococcus neoformans*. *Methods*
687 *Mol Biol* 845:165–86.
688 Soromani C, Zeng N, Hollemeyer K, Heinzle E, Klein M-C, Tretter T, et al (2012). N-
689 acetylation and phosphorylation of Sec complex subunits in the ER membrane. *BMC Cell*
690 *Biol* 13:34.

691 Srikanta D, Santiago-Tirado FH, and Doering TL (2014). *Cryptococcus neoformans*:
692 historical curiosity to modern pathogen. *Yeast* 31:47-60.
693 Stirling CJ, Rothblatt J, Hosobuchi M, Deshaies R, Schekman R (1992). Protein translocation
694 mutants defective in the insertion of integral membrane proteins into the endoplasmic
695 reticulum. *Mol Biol Cell* 3:129–42.
696 Toikkanen J, Gatti E, Takei K, Saloheimo M, Olkkonen VM, Söderlund H, de Camilli P,
697 Keränen S (1996). Yeast protein translocation complex: Isolation of two genes SEB1
698 and SEB2 encoding proteins homologous to the Sec61ß subunit**.** *Yeast* 12:425-438.
699 Tyanova S, Temu T, Sinitcyn P, Carlson A, Hein MY, Geiger T, Mann M, Cox J (2016). The
700 Perseus computational platform for comprehensive analysis of proteomics data. Nat
701 Methods 13:731-40.
702 Ubersax JA, Ferrell JE jr (2007). Mechanisms of specifity in protein phosphorylation. *Nature*
703 8:530-542.
704 Valcarcel R, Weber U, Jackson DB, Benes V, Ansorge W, Bohmann D, Mlodzik M (1999).
705 Sec61beta, a subunit of the protein translocation cannel, is required during Drosophila
706 development. *J Cell Sci* 112:4389-96.
707 Vembar SS, Jonikas MC, Hendershot LM, Weissman JS, Brodsky JL (2010). J domain co-
708 chaperone specificity defines the role of BiP during protein translocation. J Biol Chem
709 285:22484-94.
710 Voorhees R and Hegde RS (2016). Toward a structural understanding of co-translational
711 protein translocation. *Curr Opin Cell Biol* 41:91-99.
712 Vu K, Tham R, Uhrig JP, Thompson GR 3rd, Na Pombejra S, Jamklang M, Bautos JM, Gelli
713 A (2014). Invasion of the central nervous system by *Cryptococcus neoformans*
714 requires a secreted fungal metalloprotease. *MBio* 5: e01101-01114.

715 Wang ZA, Li LX, Doering TL (2018). Unravelling synthesis of the cryptococcal cell wall and
716 capsule. Glycobiology 28:719-730.
717 Washiyama M, Koizumi N, Fujii M, Watanabe Y (2014). Sec61ß regulates barrier functions
718 of tight junctions through expression of claudin-4 in MDCK cells. *Biol Pharm Bull*
719 37:979-986.
720 Wei YY, Liang S, Zhang YR, Lu JP, Lin FC, Liu XH (2020). MoSec61ß, the beta subunit of
721 Sec61, is involved in fungal development and pathogenicity, plant immunity, and ER-
722 phagy in Magnaporthe oryzae. *Virulence* 11:1685-1700.
723 Werness S, Anderson DJR (2011). Studio User Manual. Computer programs in biomedicine.
724 doi:10.1007/SpringerReference_28001
725 Wisniewski JR, Gaugaz FZ (2015). Fast and sensitive total protein and peptide assays for
726 proteomic analysis. Anal Chem 87:4110-6.
727 Wu X, *et al.* (2019) Structure of the post-translational protein translocation machinery of the
728 ER membrane. *Nature* 566:136-139.
729 Ziska A, Tatzelt J, Dudek J, Paton AW, Paton JC, Zimmermann R, Haßdenteufel S (2019).
730 The signal peptide plus a cluster of positive charges in prion protein dictate chaperone-
731 mediated Sec61-channel gating. *Biol Open* 8(3). pii:bio040691.
732
733
734
735
736
737
738
739

740 **TABLE 1**

Gene ID	Gene name	Protein function	SP or TM	WT/*sbh1Δ* proteomics [log2-fold]	Virulence citations	24 h/0 h RNA-seq
CNAG_00150		serine endoptidase, cell wall	SP1-23	5.24	Liu 2008	1.68
CNAG_01653	*CIG1*	cytokine-inducing glycoprotein	SP1-19	4.00	Cadieux 2013	385.34
CNAG_01172	*PBX1*	beta-helix containing protein	SP1-18	3.68	Liu 2008; 2007; Kumar 2014	0.78
CNAG_04735	*MPR1*	extracellular metalloproteinase (Mep1)	SP1-19	3.44	Liu 2008; Vu 2014	122.79
CNAG_00897	*SKN1*	glucosidase	TM134-58	3.04	Gilbert 2010	3.43
CNAG_02030		glyoxal oxidase	SP1-21	2.79	Liu 2008	0.97
CNAG_00600	*CAP60*	capsule-associated protein	SP1-33	2.65	Chang 1998	1.97
CNAG_01331			SP1-18	2.62	Liu 2008	13.45

741

742 **Table 1. Sbh1-dependent proteins involved in cryptococcal virulence.**

743 These proteins meet the following criteria: their expression under host-like conditions was at
744 least two-fold higher in WT compared to *sbh1Δ* cells; they contain an SP or TM domain; and
745 they are required for normal *C. neoformans* virulence in mouse infections. Note that this is
746 likely a subset of such proteins, as most cryptococcal proteins have not been tested for roles in
747 virulence; other candidates that meet the first two criteria are listed in Supplementary Table 1.
748 Proteomics results are shown as the ratio of expression in WT versus *sbh1Δ* cells under host-
749 like conditions. RNA-seq results are shown as the ratio of gene expression at 24 h versus 0 h
750 under host-like conditions (Maier et al., 2015).

751

752 # FIGURE LEGENDS

753 **FIGURE 1: Sbh1 is required for cell wall integrity in *S. cerevisiae*. A)** Structure of the
754 Sec61 channel of *S. cerevisiae* (modified from Wu et al., 2019; PDB 6ND1). The N-terminal
755 half of Sec61 is shown in blue, C-terminal half in green, Sss1 in grey, and Sbh1 in magenta.
756 The intrinsically unstructured N-terminal 38 amino acids of Sbh1 that were not visible in the
757 cryo-EM structure were drawn in by hand. P, phosphorylation sites; dashed lines, position of
758 the ER membrane; arrow, direction of protein transport. **B)** Alignment of the poorly
759 conserved N-termini of Sbh1 proteins from *S. cerevisiae* (Sbh1, Sbh2) and the following
760 pathogenic fungi: Cryn *Cryptococcus neoformans*, Sjap *Schizosaccharomyces japonicus*,
761 Hcap *Histoplasma capsulatum*, Bder *Blastomyces dermatidis*, Cpos *Coccidioides posadasii*,
762 Afum *Aspergillus fumigatus*, Anig *Aspergillus niger*, Bfuc *Botryotinia fuckeliana*, Sbra
763 *Sporothrix brasiliensis*. Except for Sbh2, only regions containing S or T residues with
764 flanking prolines (pink) are shown. The conserved proline-flanked T5 in *S. cerevisiae* Sbh1 is
765 indicated by an asterisk; other confirmed phosphorylation sites in *S. cerevisiae* Sbh1 are
766 shown in grey; and the PKA site in *C. neoformans* Sbh1 is in blue. *Schizosaccharomyces*
767 *cryophilus*, *Schizosaccharomyces octoporus*, *Ceratocystic fimbriana*, *Candida albicans*,
768 *Schizosaccharomyces pombe*, *Kluyveromyces lactis*, *Yarrowia lipolytica*, *Pichia pastoris*, and
769 *Hansenula polymorpha* Sbh1 proteins were also screened, but do not contained potential
770 proline-flanked phosphorylation sites. **C)** Wildtype *SBH1 SBH2 S. cerevisiae* and the
771 indicated mutants were grown on YPD plates at the indicated temperatures for 3 days. **D)**
772 Left: The Δ*sbh1*Δ*sbh2 S. cerevisiae* strain was transformed with pRS415 without an insert
773 (Δ*sbh1/2*), wildtype *SBH1*, or the indicated phosphorylation site mutants and grown on SC
774 without leucine containing 10 µg/ml calcofluor white at 30°C. A Δ*kre6* mutant and its
775 isogenic wildtype were included as controls. Note that these are in a different strain
776 background compared to the *SBH1* strain. Right: The indicated strains were grown to early

777 exponential phase and cell-wall proteins extracted by high pH/DTT, resolved by SDS-PAGE
778 (size range shown is roughly 10-150 kD), and visualized by Coomassie staining.
779
780 **FIGURE 2: Sbh1 is required for cell wall integrity at high temperature in *C.neoformans*.**
781 **A)** Serial 10-fold dilutions of wild-type (KN99) and Δ*sbh1* cells were grown at the
782 temperatures shown on YPD alone or containing 1 mg/ml calcofluor white (CFW) or 0.02%
783 SDS (SDS). **B)** Wild type (KN99) or *sbh1*Δ mutant cells were transformed with vector alone
784 (vec) or plasmids encoding HA-tagged Sbh1 (SBH1), or Sbh1 with mutations in the indicated
785 phosphorylation sites and then diluted as in panel A and grown at the indicated conditions. **C)**
786 Cells of the strains indicated were treated with lysing enzymes (see Methods) for the times
787 shown and then assessed for % lysis with two-way ANOVA with mixed-effects analysis. *
788 indicates $P<0.05$, # indicates $P=0.25$. **D)** The indicated strains were grown as above in the
789 presence of 1 mM H_2O_2 or 1mM $NaNO_2$ on YNB (pH 5) at 37°C. All experiments are
790 representative of at least three biological replicate studies.
791
792 **FIGURE 3: *C. neoformans* Sbh1 is required for the induction of secretory and**
793 **transmembrane proteins in host-like conditions.** Proteomic analysis of wildtype and *sbh1*Δ
794 *C. neoformans* grown in YPD at 30°C or DMEM and 5% CO_2 at 37°C (host-like conditions).
795 Samples were analyzed in quadruplicates. Gene IDs of known virulence factors are indicated
796 by asterisks.
797
798 **FIGURE 4: Secretory and transmembrane proteins that require Sbh1 for induction**
799 **contain specific ER-targeting sequences. A)** Characterization of Sbh1-dependent
800 transmembrane domains. Top, schematic of a typical transmembrane domain (TMD) with
801 features specific for Sbh1-dependent TMDs highlighted in red. Hydrophobicity (left) and

802 charges within 10 amino acids of TMDs (right) were analyzed for TMDs of Sbh1-
803 dependently induced proteins (candidates, red) compared to all transmembrane proteins in the
804 *C. neoformans* proteome (black). **B**) Characterization of Sbh1-dependent signal peptides. The
805 schematic on top shows a typical signal peptide (SP) with features specific for Sbh1-
806 dependent SPs highlighted in red. Black triangle: signal peptidase cleavage site. SPs of Sbh1-
807 dependently induced secretory proteins (red) were analyzed for N-region charge, H-region
808 hydrophobicity and length, and C-region polarity and compared to all signal peptides in the *C.*
809 *neoformans* proteome (black). The only difference found was in C-region polarity, shown in
810 the graph. **C)** Model for Sbh1 function in *C. neoformans*. Under rich medium conditions,
811 proteins with Sbh1-dependent ER targeting sequences (magenta) play only a minor role for
812 vegetative growth (left), and most proteins imported into the ER have Sbh1-independent
813 targeting sequences (shaded grey). During infection (right), however, Sbh1-dependent ER
814 import (magenta) becomes essential.
815
816 **FIGURE 5: The *C. neoformans sbh1*Δ mutant is avirulent in mouse infection.** (A, B)
817 Total fungal burden at 14 days post-infection with the indicated strains, measured in lung (A)
818 and brain (B). Each symbol represents colony forming units (CFU) for one mouse; mean and
819 standard deviation are also shown. Dotted line, original inoculum. (C) Mouse survival after
820 infection with KN99 wildtype (solid line), *sbh1*Δ (dashed line) or *sbh1*Δ complemented with
821 wildtype *SBH1* (dotted line). Any mouse that decreased to less than 80% of its initial weight
822 (see Supplementary Figure 3) was humanely sacrificed and considered not to survive the
823 infection.
824
825
826

827 # SUPPLEMENTARY INFORMATION

828 **TABLE S1 (excel file): Protein expression analysis in KN99 wild-type and *sbh1*Δ *C.***
829 ***neoformans* grown in YPD at 30°C or DMEM at 37°C and 5% CO_2.**
830 Proteins are ordered by degree of Sbh1-dependence. Where present, ER targeting sequences
831 are indicated by amino acid numbers. SP, signal peptides; SA, uncleaved signal anchors; TM,
832 first transmembrane domain. Ambiguous predictions due to limited hydrophobicity (TM) or
833 suboptimal signal peptide parameters (SP) are indicated by '?'.
834
835 **TABLE S2 (word doc): Signal peptides and transmembrane domains of proteins**
836 **induced in DMEM in KN99 wildtype *C. neoformans*.** Amino acid sequences of TM
837 domains, signal peptides, and signal anchors are shown including the flanking 10 amino acids
838 on either side for TM or the first 10 amino acids of the mature domains for SP. Positively
839 charged amino acid residues are highlighted in red.
840
841 **SUPPLEMENTARY FIGURE 1: Expression of wild type and phosphorylation mutants**
842 **of Sbh1.** Shown is an anti-HA immunoblot of wildtype or *sbh1*Δ cryptococcal cells expressing
843 either vector alone (vec) or the indicated HA-tagged proteins. This blot is representative of
844 two independent experiments.
845
846 **SUPPLEMENTARY FIGURE 2: Growth of *C. neoformans* wild-type and *sbh1*Δ under host-**
847 **like conditions.** (A) Fungi of the indicated strains were incubated in tissue culture medium (5% CO_2,
848 37 °C) and then plated on YPD for assessment of colony-forming units (CFU) after 1, 18, and 30 h.
849 Results were normalized to the 1 h CFU value. (B) The same strains were incubated for 1 h in the
850 presence of differentiated THP-1 cells (MOI = 1), during which time fungi were engulfed by the host
851 cells. Samples were then vigorously washed to remove free cryptococci and host cells were lysed to

852 measure CFU either immediately or after 30 h of incubation. % change was calculated as [(Final CFU
853 – Initial CFU) / (Initial CFU)] x 100. Results shown are mean and SEM values from 4 independent
854 experiments for (A) and 2 independent experiments for (B). For both panels * indicates $p < 0.05$ for
855 *sbh1*Δ compared to KN99.
856
857 **SUPPLEMENTARY FIGURE 3: Weight over time of mice** intranasally infected with
858 $5x10^4$ cells of wild type (blue) or *sbh1*Δ (red) cells. Dashed lines indicate 80% of the average
859 initial weight for each group, which was used to determine the time of sacrifice.
860

Figure 1

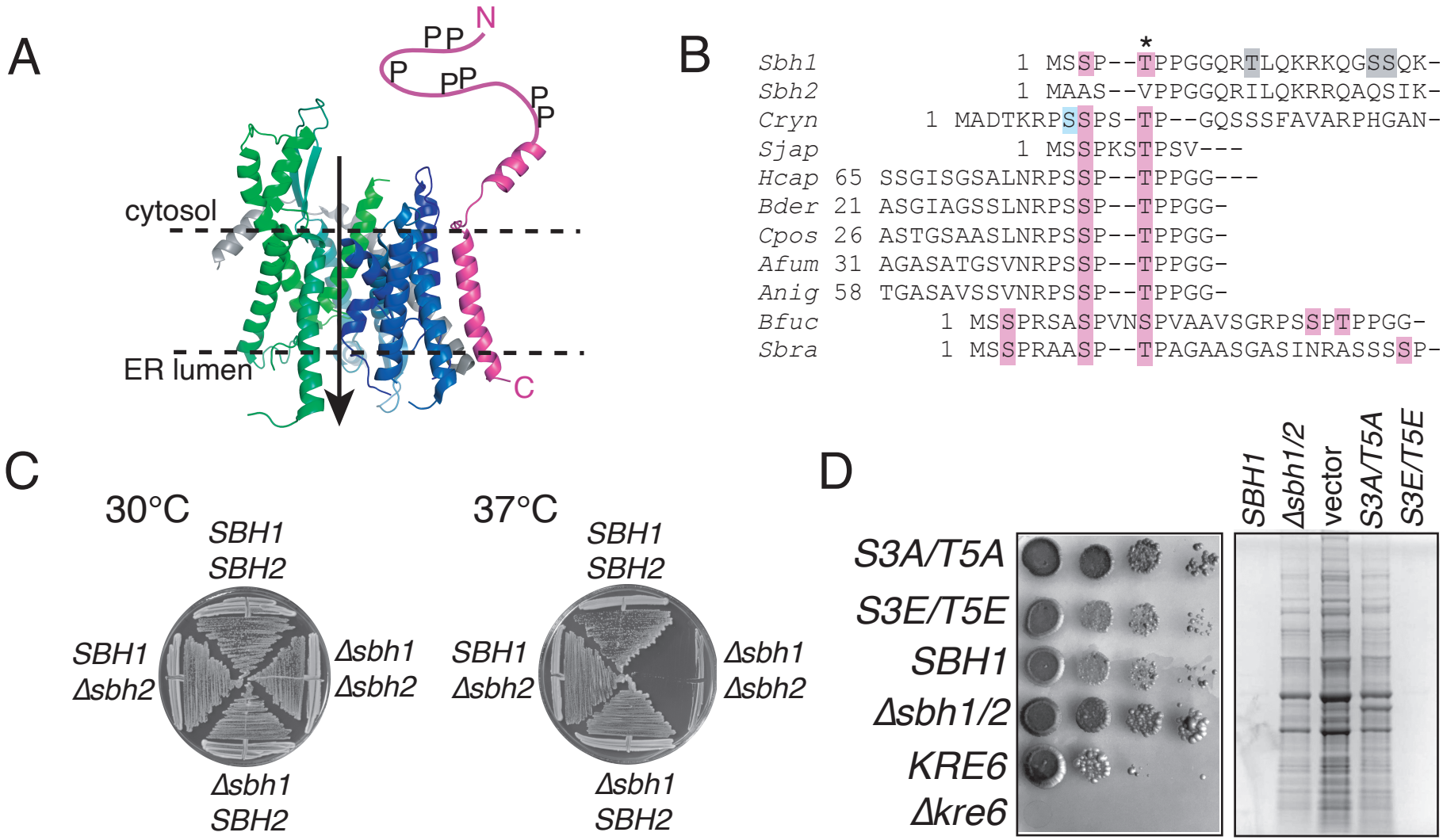
A
N
P P
P
P P
P
P
cytosol
ER lumen
C
B
*
Sbh1 1 MSSP--TPPGGQRTLQKRKQGSSQK-
Sbh2 1 MAAS--VPPGGQRILQKRRQAQSIK-
Cryn 1 MADTKRPSSPS-TP--GQSSSFAVARPHGAN-
Sjap 1 MSSPKSTPSV---
Hcap 65 SSGISGSALNRPSSP--TPPGG---
Bder 21 ASGIAGSSLNRPSSP--TPPGG-
Cpos 26 ASTGSAASLNRPSSP--TPPGG-
Afum 31 AGASATGSVNRPSSP--TPPGG-
Anig 58 TGASAVSSVNRPSSP--TPPGG-
Bfuc 1 MSSPRSASPVNSPVAAVSGRPSSPTPPGG-
Sbra 1 MSSPRAASP--TPAGAASGASINRASSSSP-
C
30°C
SBH1
SBH2
SBH1
Δsbh2
Δsbh1
Δsbh2
Δsbh1
SBH2
37°C
SBH1
SBH2
SBH1
Δsbh2
Δsbh1
Δsbh2
Δsbh1
SBH2
D
SBH1
Δsbh1/2
vector
S3A/T5A
S3E/T5E
S3A/T5A
S3E/T5E
SBH1
Δsbh1/2
KRE6
Δkre6

Figure 2

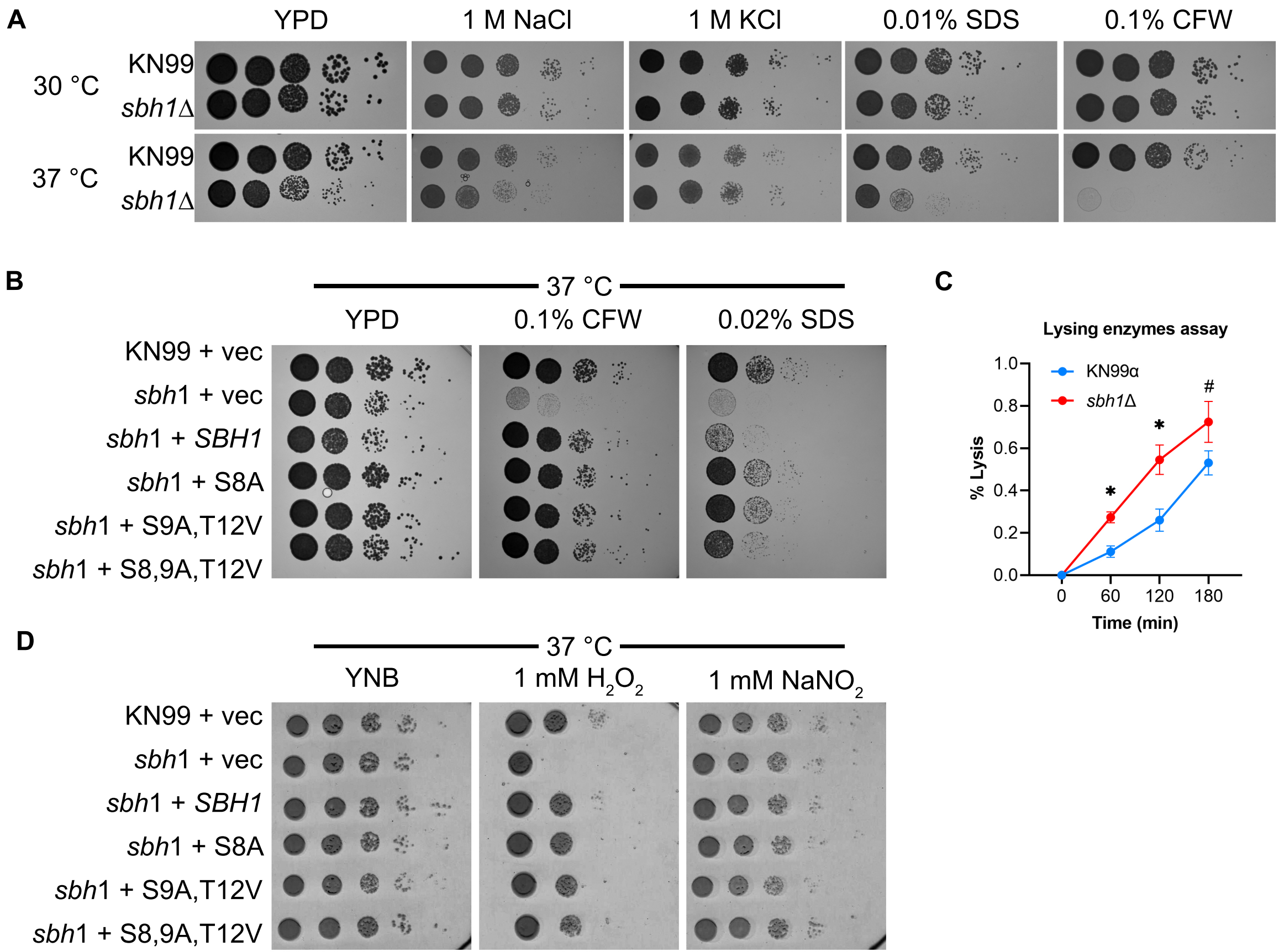
A
YPD
1 M NaCl
1 M KCl
0.01% SDS
0.1% CFW
30 °C
KN99
sbh1Δ
37 °C
KN99
sbh1Δ
B
37 °C
YPD
0.1% CFW
0.02% SDS
KN99 + vec
sbh1 + vec
sbh1 + SBH1
sbh1 + S8A
sbh1 + S9A,T12V
sbh1 + S8,9A,T12V
C
Lysing enzymes assay
KN99α
sbh1Δ
% Lysis
1.0
0.8
0.6
0.4
0.2
0.0
0
60
120
180
Time (min)
*
*
#
D
37 °C
YNB
1 mM H2O2
1 mM NaNO2
KN99 + vec
sbh1 + vec
sbh1 + SBH1
sbh1 + S8A
sbh1 + S9A,T12V
sbh1 + S8,9A,T12V

Figure 3

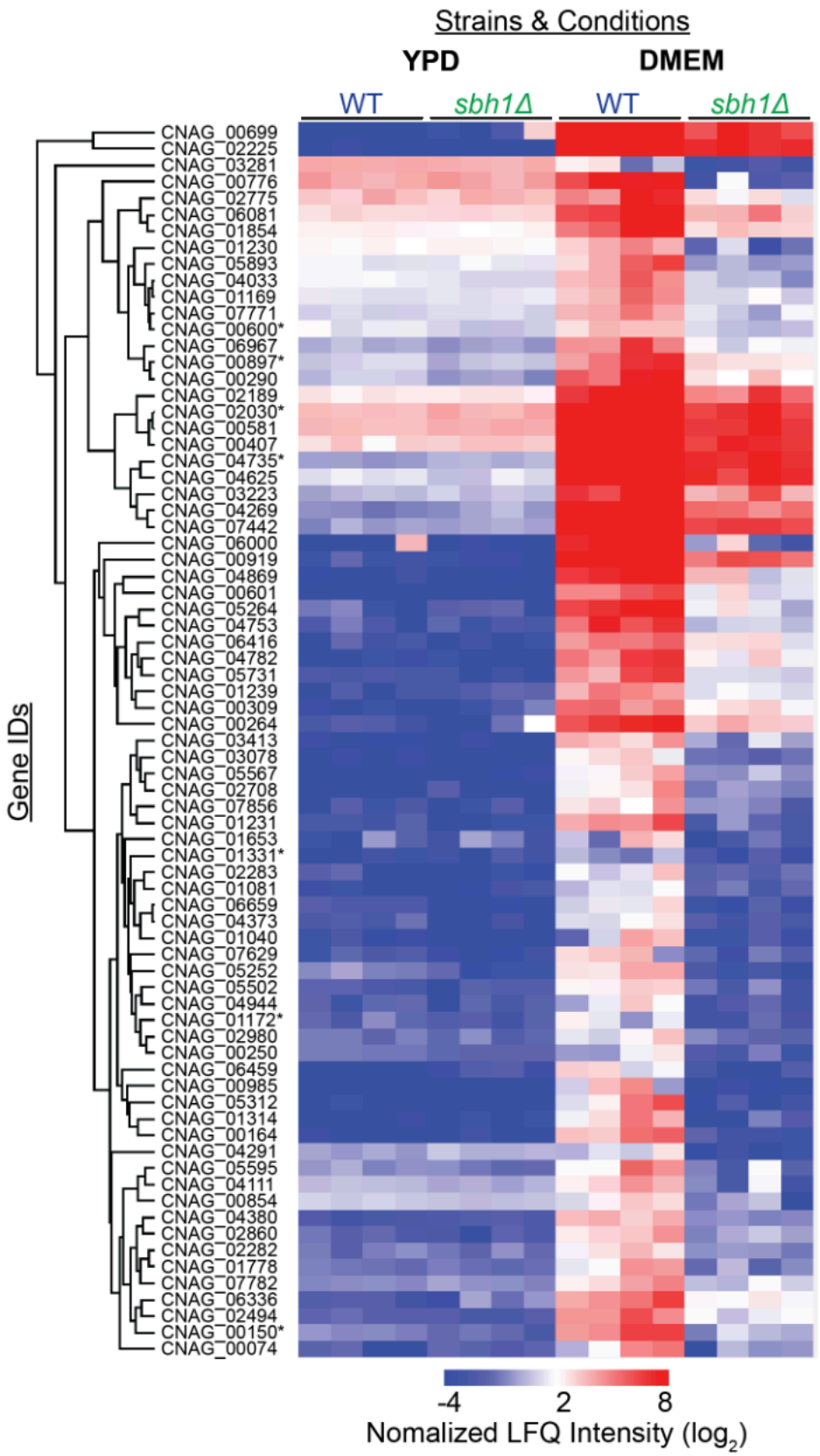
Strains & Conditions
YPD
DMEM
WT
sbh1Δ
WT
sbh1Δ
Gene IDs
CNAG_00699
CNAG_02225
CNAG_03281
CNAG_00776
CNAG_02775
CNAG_06081
CNAG_01854
CNAG_01230
CNAG_05893
CNAG_04033
CNAG_01169
CNAG_07771
CNAG_00600*
CNAG_06967
CNAG_00897*
CNAG_00290
CNAG_02189
CNAG_02030*
CNAG_00581
CNAG_00407
CNAG_04735*
CNAG_04625
CNAG_03223
CNAG_04269
CNAG_07442
CNAG_06000
CNAG_00919
CNAG_04869
CNAG_00601
CNAG_05264
CNAG_04753
CNAG_06416
CNAG_04782
CNAG_05731
CNAG_01239
CNAG_00309
CNAG_00264
CNAG_03413
CNAG_03078
CNAG_05567
CNAG_02708
CNAG_07856
CNAG_01231
CNAG_01653
CNAG_01331*
CNAG_02283
CNAG_01081
CNAG_06659
CNAG_04373
CNAG_01040
CNAG_07629
CNAG_05252
CNAG_05502
CNAG_04944
CNAG_01172*
CNAG_02980
CNAG_00250
CNAG_06459
CNAG_00985
CNAG_05312
CNAG_01314
CNAG_00164
CNAG_04291
CNAG_05595
CNAG_04111
CNAG_00854
CNAG_04380
CNAG_02860
CNAG_02282
CNAG_01778
CNAG_07782
CNAG_06336
CNAG_02494
CNAG_00150*
CNAG_00074
-4
2
8
Nomalized LFQ Intensity (log2)

Figure 4

A

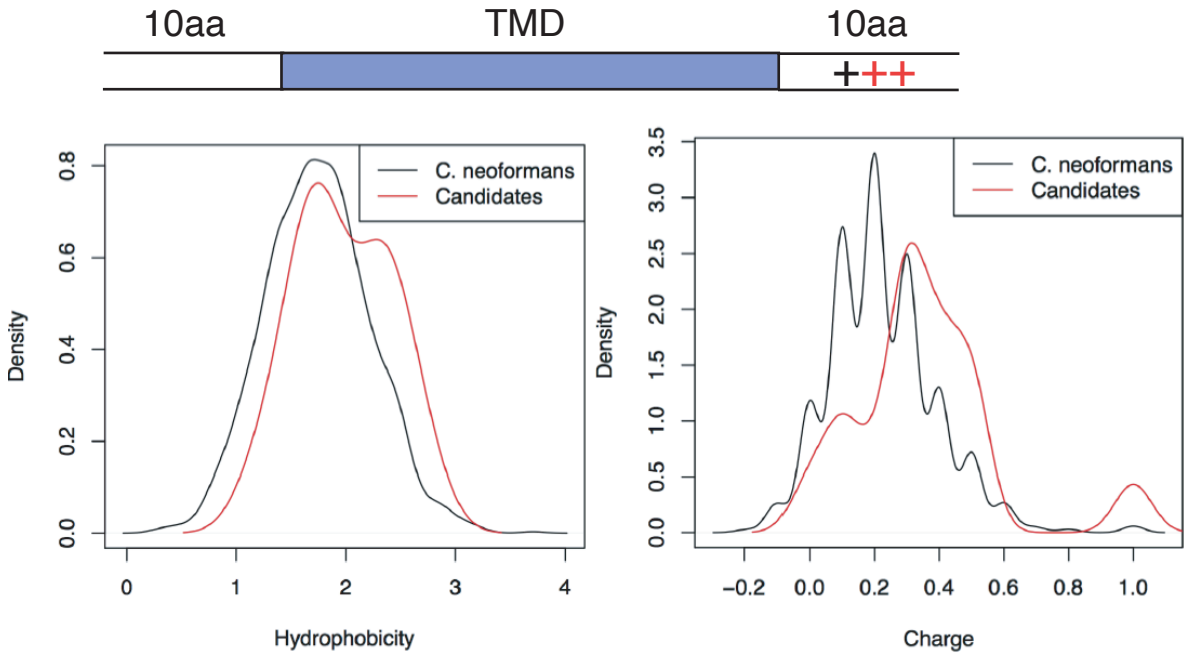
10aa
TMD
10aa
+++
C. neoformans
Candidates
Density
Hydrophobicity
Charge

B

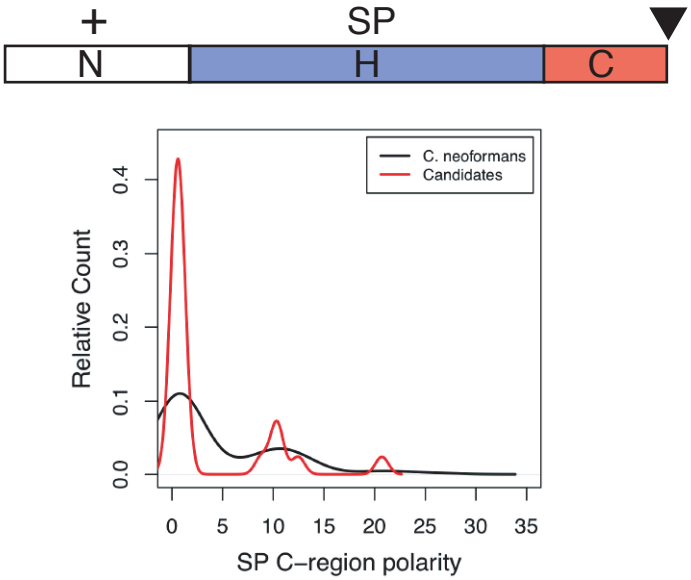
+
SP
N
H
C
C. neoformans
Candidates
Relative Count
SP C–region polarity

C

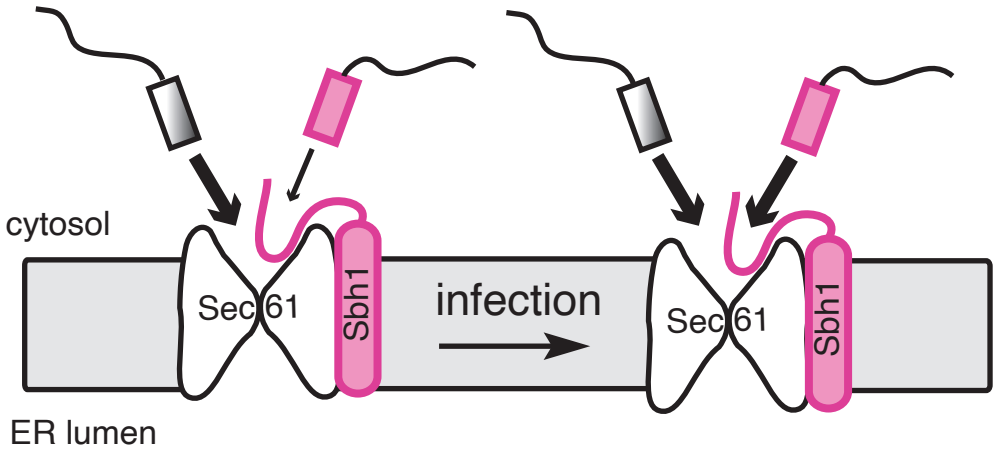
cytosol
Sec 61
Sbh1
infection
Sec 61
Sbh1
ER lumen

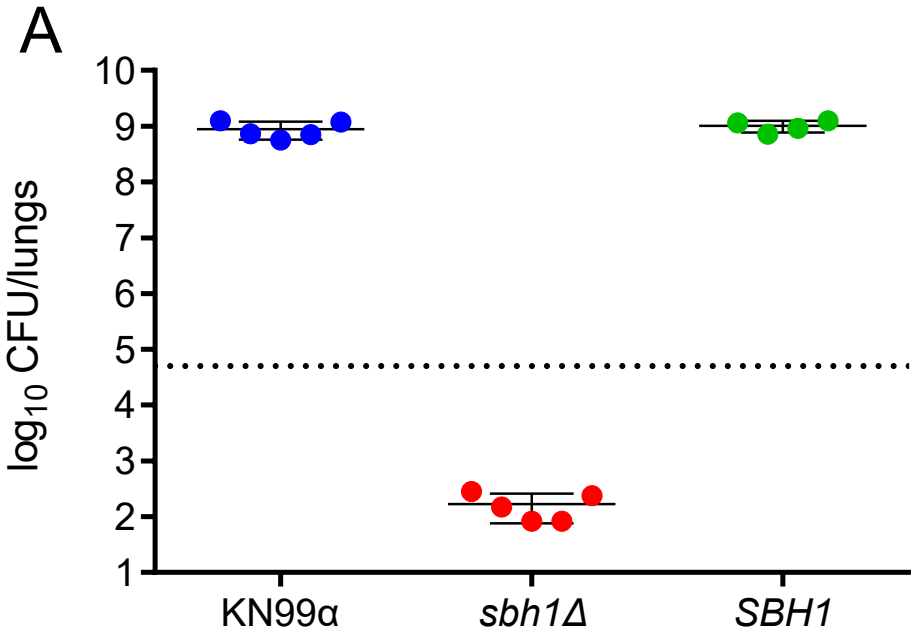
A
log10 CFU/lungs
10
9
8
7
6
5
4
3
2
1
KN99α
sbh1Δ
SBH1

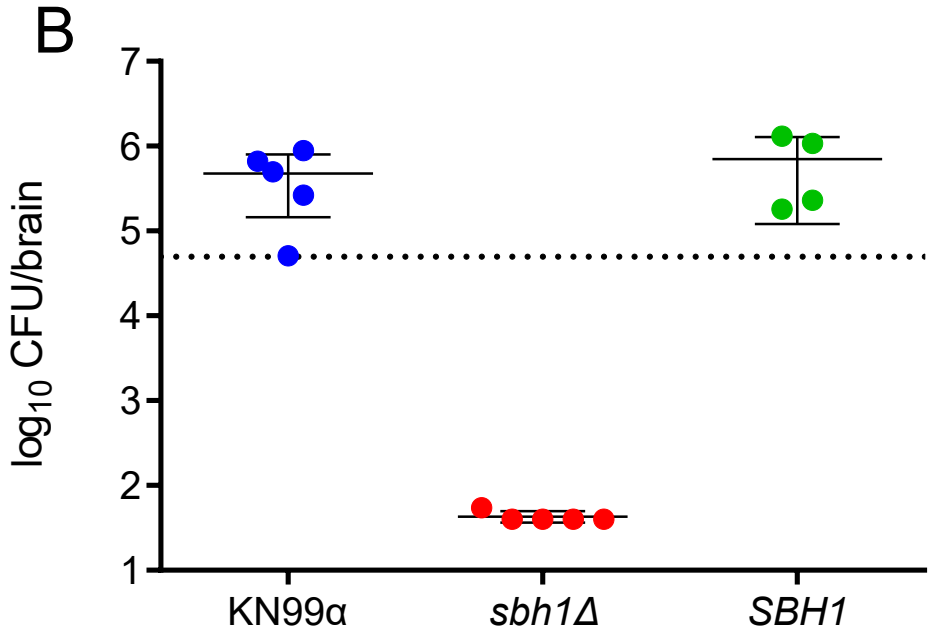
B
log10 CFU/brain
7
6
5
4
3
2
1
KN99α
sbh1Δ
SBH1

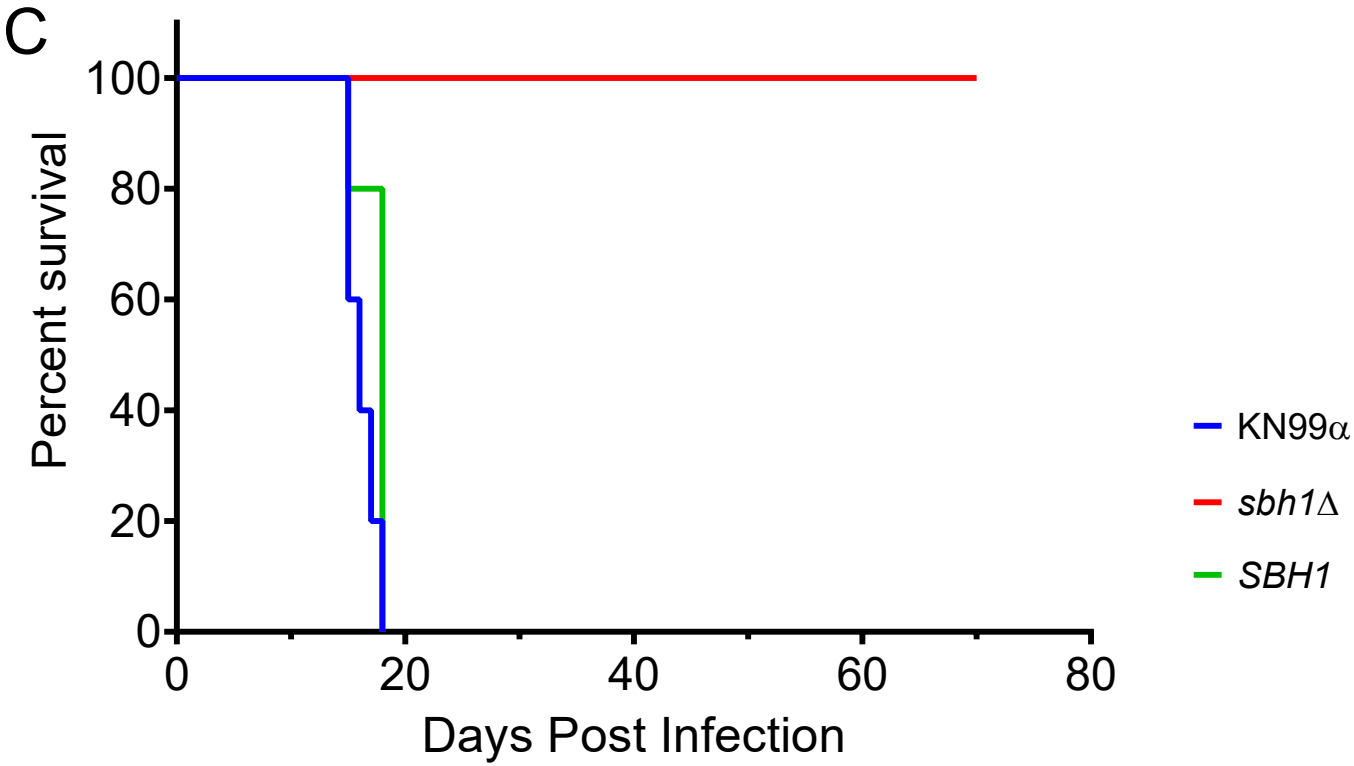
C
Percent survival
100
80
60
40
20
0
0
20
40
60
80
Days Post Infection
KN99α
sbh1Δ
SBH1